

# Protein-Protein Interactions Studied by EPR

## Relaxation Measurements: Cytochrome *c* and Cytochrome *c* Oxidase

*Sevdalina Lyubenova,<sup>#</sup>M. Khalid Siddiqui, Marloes J. M. Penning de Vries,<sup>#</sup>Bernd*

*Ludwig, Thomas F. Prisner\**

Johann Wolfgang Goethe University Frankfurt am Main, Germany

Institute of Physical and Theoretical Chemistry and Center for Biomolecular Magnetic  
Resonance

<sup>#</sup>Institute of Biochemistry

\*Corresponding author: prisner@epr.uni-frankfurt.de

### Supporting Information

#### Table of contents

A) Temperature and Orientation Dependence of Dipolar Relaxation	page S2
B) Dipolar Relaxation Traces as a Function of Cytochrome <i>c</i> Concentration	page S7
C) Temperature dependence of dipolar relaxation by cytochrome <i>c</i> <sub>1</sub>	page S9

## A) Temperature and Orientation Dependence of Dipolar Relaxation

The temperature dependence of the dipolar relaxation rate  $1/T_2^{\text{dip}}$  is a direct result of the temperature dependence of the longitudinal relaxation time of the fast relaxing  $\text{Fe}^{3+}$  spin of cytochrome *c* ( $T_1^{\text{cyt}}$ ).<sup>31</sup> Two regions have to be distinguished: the low temperature region (with  $T_1^{\text{cyt}} \cdot \Delta > 1$ ) and the high temperature region (with  $T_1^{\text{cyt}} \cdot \Delta < 1$ ), where  $2\Delta$  is the dipolar splitting. A maximum in the dipolar relaxation rate  $1/T_2^{\text{dip}}$  exists for  $T_1^{\text{cyt}} \cdot \Delta = 1$  (see Figure S1).

In the low temperature region the dipolar relaxation time  $T_2^{\text{dip}}$  equals  $T_1^{\text{cyt}}$ . Hence a mono-exponential decay is expected, that becomes faster if the temperature is increased. In the high temperature region the dipolar relaxation rate is given by  $1/T_2^{\text{dip}} = \Delta^2 \cdot T_1^{\text{cyt}}/2$ . In this case a slower decay is expected with increasing temperature. Additionally, the relaxation rate here depends on the dipolar coupling strength  $\Delta$ . The dipolar coupling depends on the orientation of the vector  $R$  with respect to the external magnetic field  $B_0$ :  $\Delta(\theta) = \Delta_{\perp} (1 - 3\cos^2 \theta)$ , with  $\theta$  the angle between  $R$  and  $B_0$ , and  $2\Delta_{\perp}$  the dipolar splitting for  $R$  perpendicular to the external magnetic field. For randomly oriented molecules with a fixed distance  $R$  this orientation dependence of  $\Delta$  leads to the well-known Pake pattern distribution (see Figure S2).

In the high temperature region randomly oriented samples therefore exhibit a multi-exponential decay. This is schematically illustrated for three selected orientations:  $\theta = 90^\circ$  (A),  $54.7^\circ$  (B) and  $0^\circ$  (C). Spin pairs with an angle  $\theta = 0^\circ$  (C) have a 4-fold faster dipolar decay than molecules with an angle  $\theta = 90^\circ$  (A). Spin pairs with the interconnecting vector  $R$  at the magic angle (B) are not affected by dipolar relaxation.

The echo decay traces for these three particular orientations and their sum are illustrated in Figure S3. For the simulations of the experimental results the summation was performed over all orientations that were excited by the microwave pulses with the corresponding amplitudes.

The dotted line in Figure S3 symbolizes the shortest observable time because of experimental dead time. This leads to distortions in the relative intensities of molecules with a large dipolar coupling (C) compared to spin pairs with smaller dipolar coupling (A). If different R exist, as for the protein-protein complex, this will lead to a reduced contribution of the spin pairs with shorter distances.

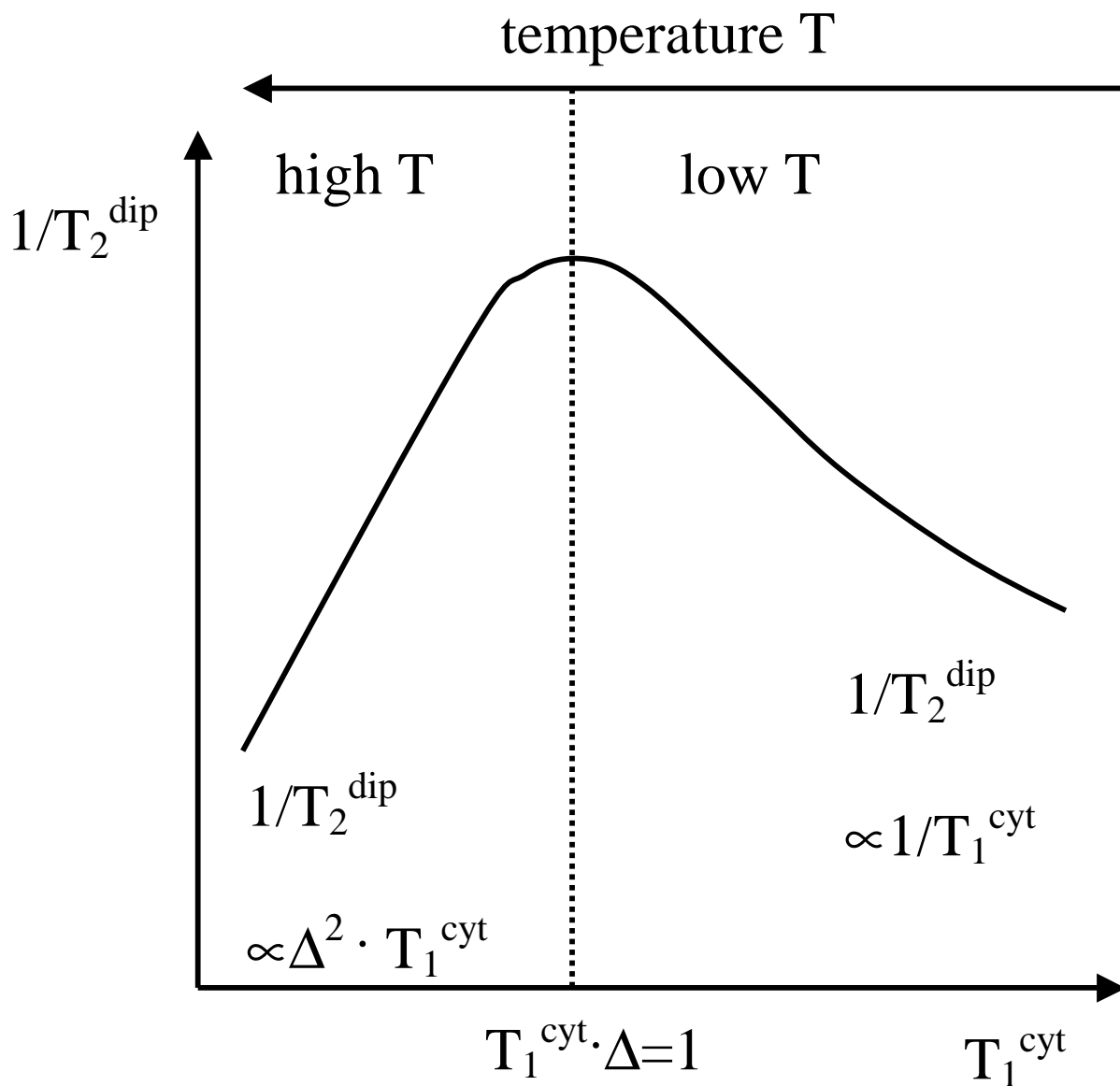


Figure S1: Schematic representation of the dipolar relaxation rate  $1/T_2^{\text{dip}}$  as a function of the cytochrome *c* relaxation time  $T_1^{\text{cyt}}$ .

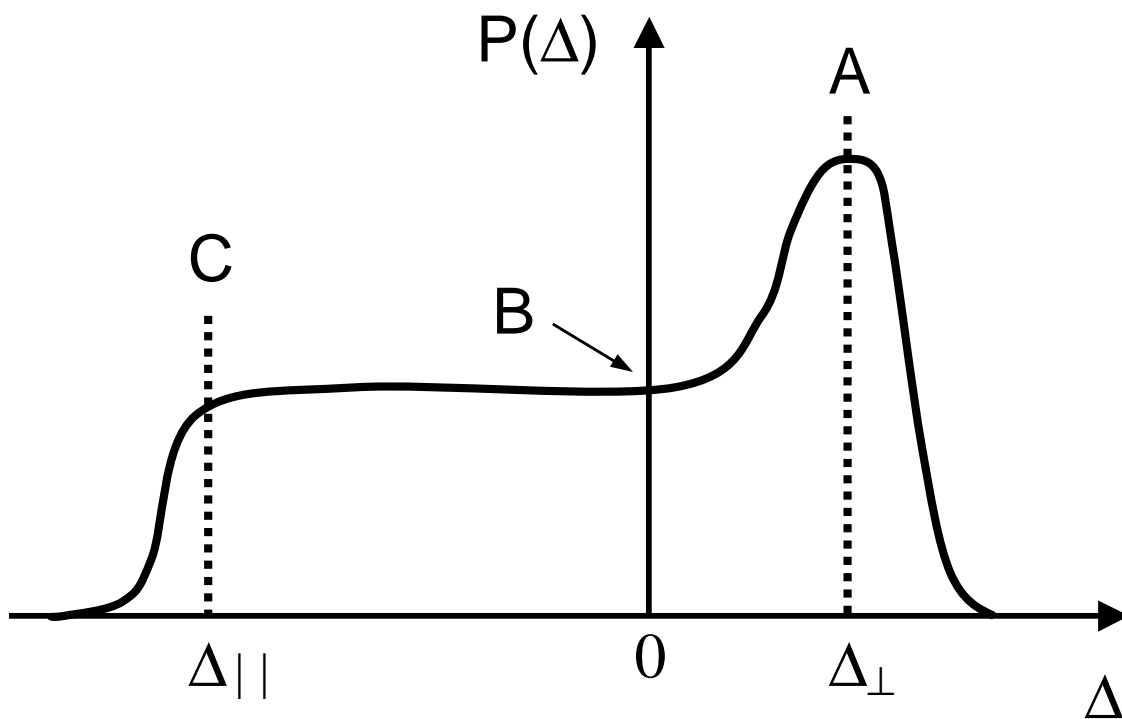


Figure S2: Pake pattern distribution of dipolar couplings for a randomly oriented sample. A, B and C correspond to  $\theta = 90^\circ$ ,  $54.7^\circ$  and  $0^\circ$  respectively.  $P(\Delta)$  is the relative number of spins experiencing a certain  $\Delta$ .

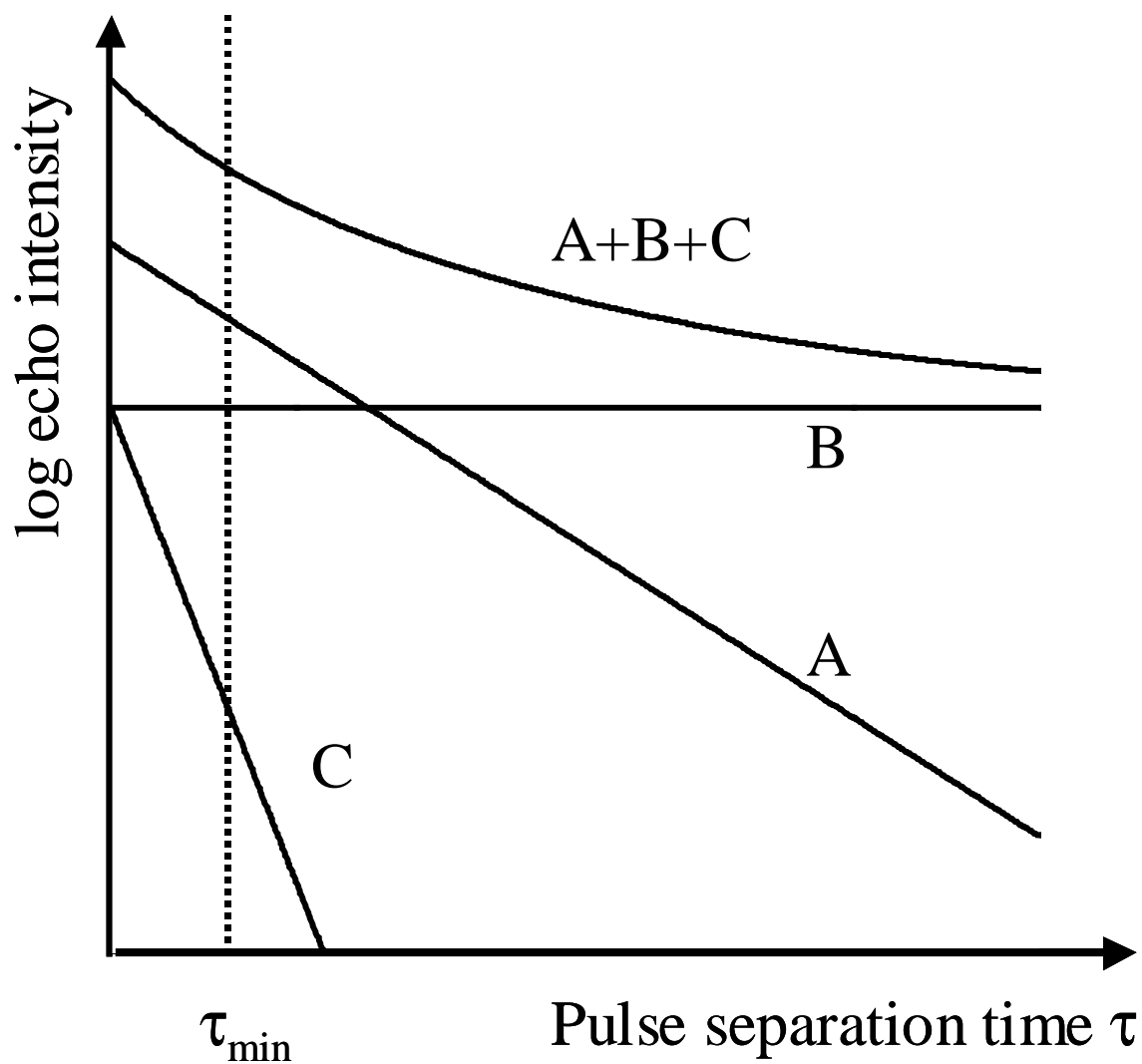


Figure S3: Hahn echo decay traces for spin pairs A, B and C with the dipolar couplings as defined in Figure S2. The sum A+B+C demonstrates the multi-exponential behavior in such disordered samples. The dotted line reflects the minimum detectable pulse separation time.

## B) Dipolar Relaxation Traces as a Function of Cytochrome *c* Concentration

To understand the concentration dependence of the dipolar relaxation traces of the Cu<sub>A</sub> center in CcO<sub>II</sub> two effects have to be taken into account: a) the intramolecular dipolar relaxation resulting from cytochrome *c* bound into a protein-protein complex, and b) the intermolecular relaxation by the other cytochrome *c* molecules randomly distributed in the frozen sample. The total experimentally observed dipolar relaxation time trace can be written as:

$$\Phi_{\text{tot}} = a \cdot \Phi_{\text{intra}} \cdot \Phi_{\text{inter}}(c) + b \cdot \Phi_{\text{inter}}(c) = (a \cdot \Phi_{\text{intra}} + b) \cdot \Phi_{\text{inter}}(c)$$

where *a* and *b* are the amount of complexed and uncomplexed CcO<sub>II</sub> protein, and *c* is the cytochrome concentration.

As explained in the paper, the dipolar relaxation of Cu<sub>A</sub> in the presence of *c*<sub>1</sub> represents the intermolecular dipolar interaction. Consequently, these relaxation traces were used to remove the intermolecular contribution from the time traces of CcO<sub>II</sub> with *c*<sub>552</sub>. In figure S4 the dipolar relaxation traces of CcO<sub>II</sub> in the presence of different concentrations of cytochrome *c*<sub>552</sub> are shown, after removal of the corresponding intermolecular relaxation contribution. For sample A, where the concentration of *c*<sub>552</sub> is half of that of CcO<sub>II</sub>, 0.5 was subsequently subtracted to account for the amount of unbound CcO<sub>II</sub>. The resulting A\* trace overlaps the B trace, as shown in figure S5.

If the cytochrome *c* concentration exceeds the CcO<sub>II</sub> concentration, the intramolecular dipolar relaxation reaches a saturation level. Hence, traces B and C should be identical if all CcO<sub>II</sub> in sample B is bound to *c*<sub>552</sub>. However, the traces do not overlap, and from this difference it was deduced that the complex yield was about 90% in sample B.

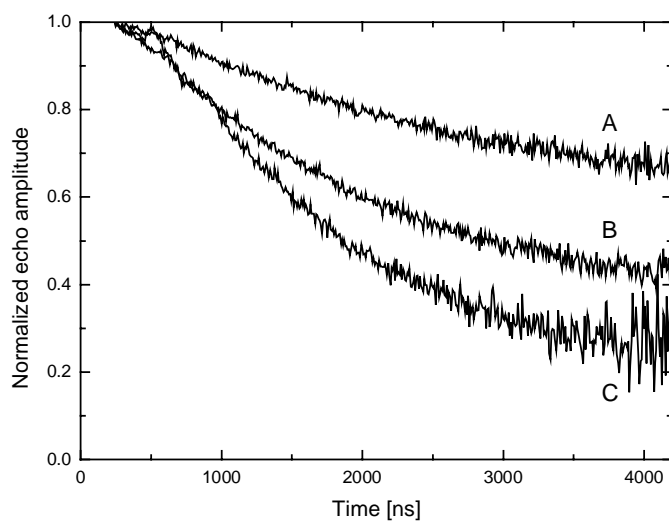


Figure S4: Dipolar relaxation traces of mixtures of  $CcO_{II}$  (100  $\mu M$ ) with  $c_{552}$  concentrations of 50  $\mu M$  (A), 100  $\mu M$  (B) and 500  $\mu M$  (C) respectively. The corresponding intermolecular relaxation contributions were removed as described in the text.

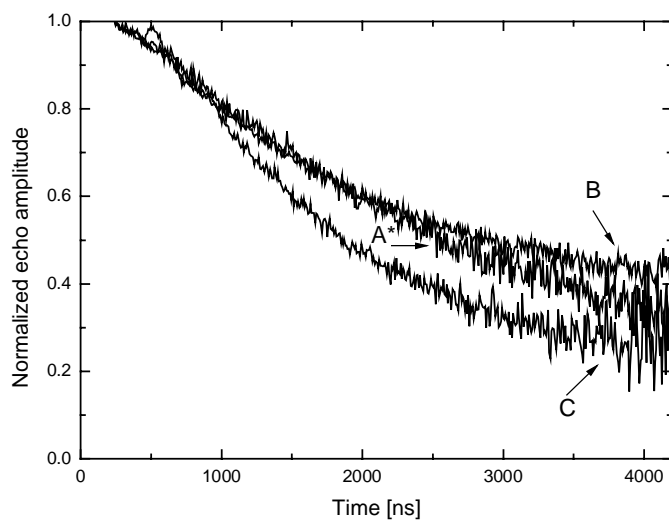




Figure S5: Dipolar relaxation traces of the  $\text{CcO}_{\text{II}}$  and  $c_{552}$  protein mixtures after removing the corresponding intermolecular relaxation contributions (A\*, B, C). In case of trace A\* 0.5 was taken off. Protein concentration as given in Figure S4.

### C) Temperature dependence of dipolar relaxation for cytochrome $c_I$

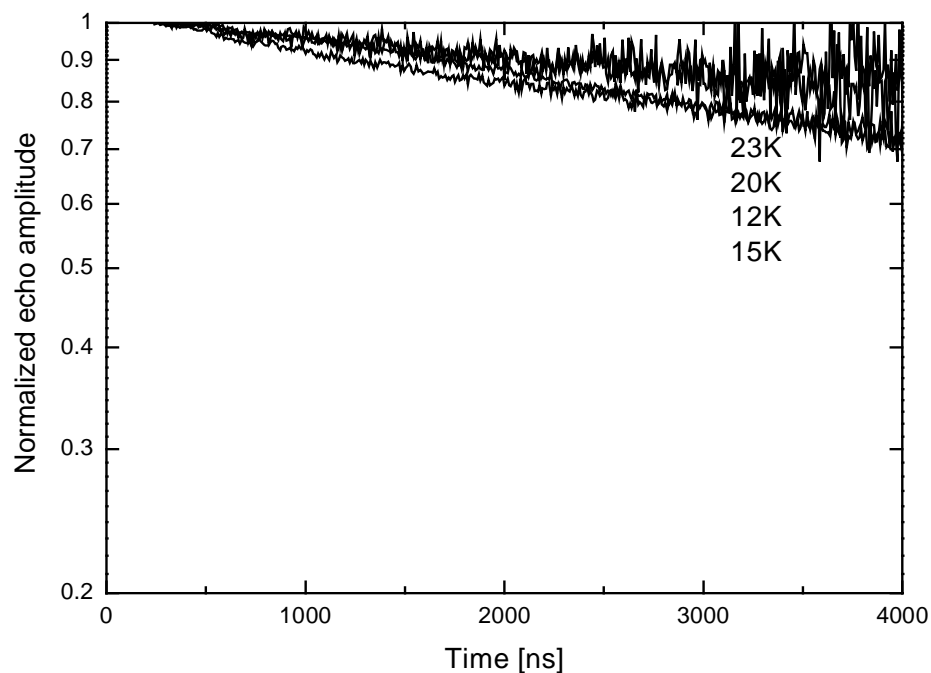


Figure S6: Semi-logarithmic plot of the dipolar relaxation traces of 100  $\mu\text{M}$  : 100  $\mu\text{M}$  mixture of  $\text{CcO}_{\text{II}}$  with  $c_I$ , measured at different temperatures as indicated in the plot. Experimental parameters as in Figure 2 in the paper. To simplify the comparison with temperature dependent measurements of the binding cytochromes, and to illustrate the very different behavior, the figure is shown with the same axis scales as Figures 4 and 5 of the paper.